Proceedings of the 25th Annual International Conference of the IEEE EMBS
Cancun, Mexico • September 17-21, 2003

M-mode Echocardiography Image and Video Segmentation based on AM-FM Demodulation Techniques

P. Rodríguez V.[1], M. S. Pattichis[1], M. B. Goens MD[2]
[1]Department of Electrical and Computer Engineering, University of New Mexico, NM, USA
[2]Children Hospital Heart Center Department of Pediatrics, UNM School of Medicine, NM, USA

Abstract—**A novel methodology to automatically segment all the walls present in M-mode echocardiography images in order to determine the ventricular chamber dimensions and wall thickness is proposed using Amplitude-Modulation Frequency Modulation (AM-FM) demodulation techniques. Preliminary results show method's capability to segment the Left Ventricular Posterior wall and the left ventricular side of the Interventricular Septum. Using these results three measurements are possible: Left Ventricular Posterior Wall (LVPW) thickness, Left Ventricular Dimension (LVDD) at end-diastole and Left Ventricular dimension (LVSD) at end-systole.**

Keywords—**AM-FM demodulation, M-mode echocardiography segmentation**

I. Introduction

Ultrasound imaging dominates diagnostic imaging in pediatric cardiology. In particular, M-mode echocardiography leads to more accurate measurements of small cardiac structures in patients with with very rapid heart rates (i.e. infant patients). For heart function assesment, it is important to be able to delineate cardiac wall boundaries, in order to be able to estimate different dimensions associated with heart function assesment.

In the present paper a novel method is proposed and developed to automatically segment cardiac walls present in M-mode echocardiography images without any manual interaction from the users. The cardiac walls include the anterior right ventricular wall, the interventricular septum walls and the left ventricular posterior wall. Using the segmented walls, five clinical measurements can be made for the assessment of heart function as shown in fig. 1: Right ventricular dimension at end-systole (RVDD), septal thickness at end-diastole (Sept), left ventricular dimension at end-systole (LVSD), left ventricular dimension at end-diastole (LVDD) and the left ventricular posterior wall thickness measure at end-diastole (LVPW).

The proposed method is based on AM-FM demodulation, which models the input image (in general, any N-dimensional signal) as a linear combination of positive amplitude functions and sinusoids with non-linear phase functions. The AM-FM demodulation has been successfully used in segmentation problems such as fingerprint identification [3] and plaque detection in ultrasound images of the Carotid artery [8]. In M-mode echocardiography images (or videos), high frequency modulation components are found in the vertical direction (changes in the image's contrast), whereas frequency modulation in the horizontal direction is less significant. The AM-FM demodulation can take advantage of this observation to track the walls' boundaries because it can adaptively select a filter which emphasizes the image's contrast change level at a given region of the input image. Applying AM-FM demodulation can be a very computationally intensive method. To address this issue, a fast implementation, using the single instruction multiple data (SIMD) components in general-purpose architectures, is developed (see section II).

This paper is organized as follows: in section II the mathematical description of the AM-FM demodulation is presented, as well as the description of its fast SIMD-based implementation and the final segmentation algorithm. In section III, preliminary results are shown, and the clinical impact is also addressed. Finally in section IV, concluding remarks are given.

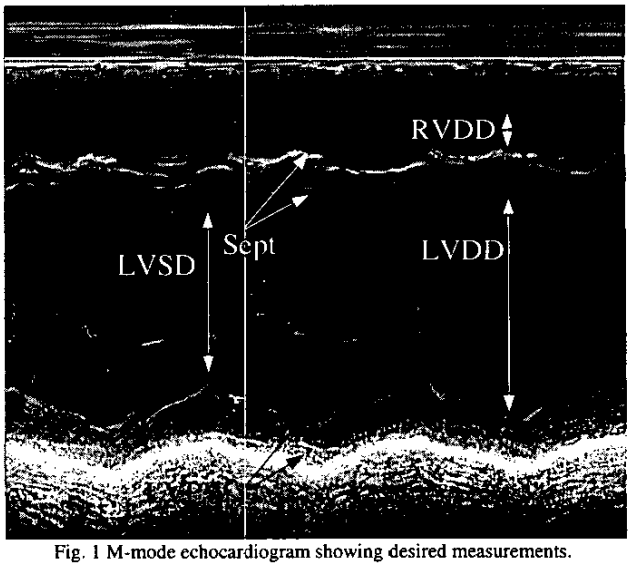

Fig. 1 M-mode echocardiogram showing desired measurements.

II. Methodology

A. AM-FM Demodulation

The so-called dominant AM-FM component describes a digital image/video in terms of:

$$\hat{X}(n_1,n_2)=\sum_{k=1}^{L} I_{[m(a)=k]}\, a_k(n_1,n_2)\cos(\varphi_k(n_1,n_2)) \quad (1)$$

where $\hat{X}(n_1,n_2)$ is the reconstructed version of the input using L different bandpass filters (see below). In (1), $X(n_1,n_2)$, n_1 is used for indexing the rows and n_2 for indexing the columns; $I_{[.]}$ is the indicator function and:

$$a(n_1,n_2)=\max\{a_k(n_1,n_2): k\in[1,L]\} \quad (2)$$

$$m(a(n_1,n_2))=\{k: a_k(n_1,n_2)=a(n_1,n_2)\} \quad (3)$$

The AM-FM demodulation algorithm operates on the analytic version of the input image:

$$X_A(n_1,n_2)=X(n_1,n_2) + j\,\mathbf{H}\{X(n_1,n_2)\} \quad (4)$$

where $\mathbf{H}\{.\}$ is the discrete hilbert transformer which operates over the rows or columns of $X(n_1,n_2)$ (see [3, 6] for details); then the amplitude $a_k(n_1,n_2)$ and phase $\varphi_k(n_1,n_2)$ are estimated from the outputs of L bandpass (complex) filters: $h_1, h_2, .. h_L$:

$$X_{Ak}=X_A * h_k \quad (5)$$

$$\varphi_k(n_1,n_2)=\arctan\left(\frac{\text{imag}(X_{Ak}(n_1,n_2))}{\text{real}(X_{Ak}(n_1,n_2))}\right) \quad (6)$$

$$a_k(n_1,n_2)=\left|\frac{X_{Ak}(n_1,n_2)}{H_k(\nabla(\varphi_k(n_1,n_2)))}\right| \quad (7)$$

$$\nabla(\varphi_k(n_1,n_2))=\text{real}\left(\frac{\nabla(X_{Ak}(n_1,n_2))}{j\,X_{Ak}(n_1,n_2)}\right) \quad (8)$$

where $\nabla(\varphi_k(n_1,n_2))$ is the instantaneous frequency and H_k is the frequency response of the filter h_k.

Even though AM-FM demodulation is a computational intensive operation, a fast implementation is possible if it is noted that the operations described in (2), (5)-(8) (with the exception of the *arctan*) can take advantage of the Single Instruction Multiple Data (SIMD) architecture, which is embedded in most current microprocessor (i.e: Motorola's PPC 74xx; Intel's PIII, P4, Itanium; AMD's Duron, Athlon, Opterom etc.). The SIMD architecture has been already used to boost the time-performance of well-known algorithms [4, 5].

B. SIMD Compliant AM-FM Demodulation

The SIMD execution model operates over *packed data* elements which could be located in memory or in a SIMD register; A *packed data* element is a vector with *S* contiguous elements; let *S*=4 (state of the art for single precision floating point numbers), and $X = [x_0\ x_1\ x_2\ x_3]$ and $Y = [y_0\ y_1\ y_2\ y_3]$ be two *packed data* elements; also let ***op*** be a SIMD math operation. Then the SIMD operation is represented by:

$$Z = X\,\mathbf{op}\,Y = [x_0\,\mathbf{op}\,y_0\ \ x_1\,\mathbf{op}\,y_1\ \ x_2\,\mathbf{op}\,y_2\ \ x_3\,\mathbf{op}\,y_3] \quad (9)$$

The AM-FM demodulation is a computational intensive operation, mainly because a collection of 2D Gabor bandpass filters are normally used in (5). An FFT based approach is a partial solution [9] to this problem because the size of the input 2D matrix is restricted to powers of two. In a more general setup a spatial convolution based approach is needed. In order to accomplish this a collection of 2D separable (into 1D) filters is preferred. A 2D Gabor filter can be then decomposed into a product of two 1D Gabor filters to speed-up the convolution needed in (5). In general, as long as the passband of interest is covered, any collection of well-defined 2D (separable) bandpass filters can be used (the optimality showed by a Gabor filter in a continuous AM-FM demodulation is lost in the discrete case).

Also, the pre-computation of the Analytic Image has a great impact in both (i) the speed-up of the AM-FM demodulation, because it allows the use of small length (number of coefficients) filters to compute (5) and (ii) in (4) the so called 'Analytic Image' is needed to avoid ambiguity when estimating the instantaneous amplitude and phase (or frequency) in (6)-(8) (see [3, 6] for details). The 'Analytic Image' is obtained by computing the 1D discrete Hilbert transform over rows or columns; this can be done by convolving the FIR Hilbert transformer with the rows or columns; a standard approach is to use the Kaiser window approximation to compute the coefficients of an M order FIR Hilbert transformer as:

$$g_{HT}(n)=(1-I_{[n=0]})\frac{2}{n\pi}\sin^2\left(\frac{n\pi}{2}\right)\quad n\in[-M,M] \quad (10)$$

From equations (1)-(8) four math operations are needed: (i) convolution (real and complex) in equations (4-5) and (8); note that the discrete gradient operator can be interpreted as a convolution; (ii) point-wise maximum value from a set of L matrices (equation (2)); (iii) pointwise multiplication and/or division of two matrices (equations (6)-(8)); and (iv) the arctan operation (eq. (6)); All these math operations (with the exclusion of the arctan function) are built-in functions in any SIMD architecture implementation. Pointwise multiplication/division and maximum of two (or more) arrays of ordered elements are directly mapped into packed operations (note that this condition is true for equations (2) and (6)-(8)). Nevertheless, a SIMD compliant convolution is not. This is addressed next.

Let $X = [x_0\ x_1\ ..\ x_{N-1}]$ be a vector with N scalar elements; also let $G = [g_0\ g_1\ ..\ g_{M-1}]$ be a filter with M scalar elements; then the linear convolution $Y = X*G$, where $Y = [y_0\ y_1\ ..\ y_{N+M-2}]$ is defined in eq. (11). Let $X_M(k) = [\,0_k\ X\ 0_{M-k-1}\,]$, where 0_N is a vector of zeros with N elements. Then eq. (11) can be rewritten as eq. (12).

$$y_n=\sum_{k=0}^{M-1} g_k\, x_{n-k} \quad (11) \qquad Y=\sum_{k=0}^{M-1} X_M(k)\, g_k \quad (12)$$

Note that convolution, as described in (12), can easily take advantage of (SIMD) packed operations: the vector $X_M(k)$ is linearly accessed and multiplied by a scalar. Then a set of M vectors are accumulated (and are linearly accessed). Also, this procedure leads to a transposition-free algorithm that can be applied to any higher dimension. Details can be found in [4].

C. *Segmentation Procedure*

The segmentation of the M-mode echocardiogram is implemented in three consecutive steps:

I. AM-FM demodulation for obtaining regions of interest (near-field, interventricular Septum, and boundary between LVPW and epicardium).
II. AM-FM demodulation for boundary extraction (interventricular septum and the left posterior ventricular wall).
III. Compute final segmentation results using energy minimization.

For step 1, a very low-frequency (in both directions) bandpass filter is used so as to get a coarse approximation of regions of interest (see section II.b). In step 2, high-frequency filtering in the vertical direction is used for extracting the wall boundaries. In both steps 1 and 2, an FM reconstruction of the original image is computed using multiple harmonics:

$$\hat{X}_L(n_1,n_2)=\sum_{k=1}^{L}\cos(k\,\varphi(n_1,n_2)) \qquad (13.a)$$

$$\hat{X}_L(n_1,n_2)=-0.5+\left(\frac{\sin(\frac{1+2L}{2}\varphi(n_1,n_2))}{2\sin(\frac{\varphi(n_1,n_2)}{2})}\right) \qquad (13.b)$$

The reconstructed image is binarized using a threshold that is a convex combination of the minimum and maximum value of $\hat{X}_L(n_1,n_2)$. Note that the maximum value of $\hat{X}_L(n_1,n_2)$ is L, and its minimun is attained when $\varphi(n_1,n_2)$ is equal to $3\pi/(2L+1)$. This scheme leads to an erosion operator (which depends on the number of harmonics used in the reconstruction, see proof in [7]), which is then used to compute the regions of interest (ROI) in the input image (see [1]).

The output of step 2 is a set of curves $C_k(n1,n2)$ and a small ROI R_k around the curve C_k, which defines the boundaries of the interventricular septum and the left posterior ventricular wall. Due to the sinusoidal shape of the walls present in M-mode echocardiography, this curve is restricted to be a linear combination of E cosine functions, where E depends on energy constrains. A local search (in region R_k) which minimizes the curve energy, as well as the potential energy of the input image, is performed to find an accurate estimate of the walls' boundaries; this is an energy minimization formulation of a deformable open contour. If after the local search, the resulting curve (boundary) does not meet a smoothness condition it is drop and the boundary is marked as missed.

III. Pre-elimanry Results

The dataset used in the present work were two M-mode echocardiography videos (10 seconds each) and a single image acquired using the ultrasound device capabilities (Sequoia, Acuson C256. Mountain View, CA 94043). The videos were acquired using a Matrox framegrabber connected to the analog video output of the Acuson. In each case, the frequencies of the ultrasound probes were: 6.5 MHz and 4.0 MHz for the digitized videos and 7.0 MHz for the single image.

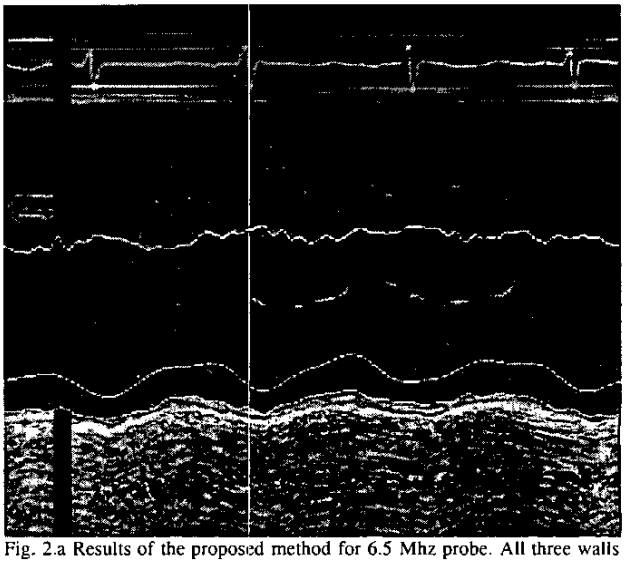

Fig. 2.a Results of the proposed method for 6.5 Mhz probe. All three walls are correctly tracked: the ventricular posterior walls and the interventricular septum wall.

The tracking properties of the preliminary results of the proposed method (see figures 2.a – 2.c) varies depending on the probe frequency. The proposed method was aimed to be a general one, to be applicable to a wide range of probe frequencies and settings. Ongoing work is focused on a detailed study of the effectiveness of the proposed methods using different settings and probes.

Fig. 2.a shows well-defined boundaries for the left ventricular wall and between blood-pool and the Septum. It must be noted that measurements such as LVPW, LVSD and LVDD can be easily made from the segmented walls. The input image is a frame taken from a 10 seconds M-mode video (ultrasound device was set to use 6.5 Mhz.). In fig. 2.b, the M-mode image was acquired using the original ultrasound device capabilities (probe frequency was 7.0 Mhz). In fig 2.b, the walls' boundaries of the left ventricle

are correctly segmented but the boundary between the blood-pool and Septum is mark as missed. In the case of fig. 2.c (original M-mode is a frame from a 10 seconds video, with the ultrasound device set to use 4.0 Mhz.) the boundary between the blood-pool and the Septum is nicely segmented, but left ventricle wall's boundaries are marked as missed.

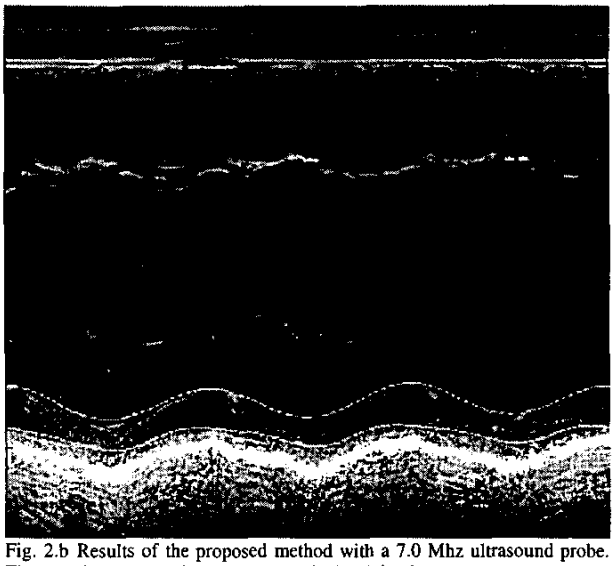

Fig. 2.b Results of the proposed method with a 7.0 Mhz ultrasound probe. The ventricular posterior walls are tracked efficiently.

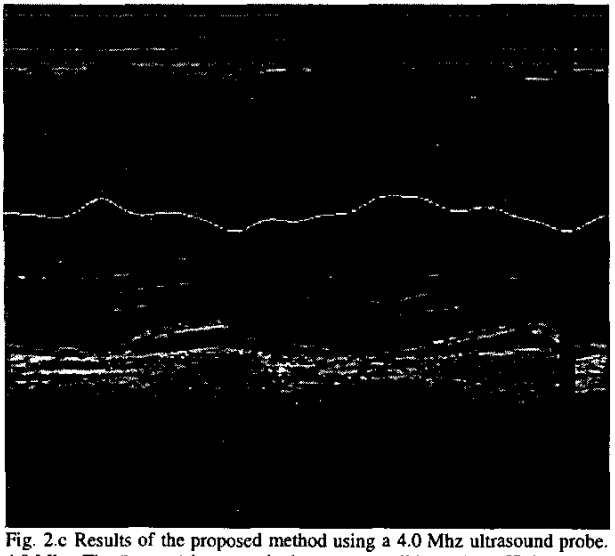

Fig. 2.c Results of the proposed method using a 4.0 Mhz ultrasound probe. 4.0 Mhz. The (bottom) interventricular septum wall is tracked efficiently.

V. Conclusion

The results indicate that the proposed method can be automated for segmenting/tracking a variety of wall boundaries, under a variety of settings. However, a detailed study on the algorithms performance for a number of probe frequencies and gain settings is currently ongoing. The proposed methods' results also show robustness with respect to the image acquisition method.

A novel mathematical morphology operator based on the AM-FM demodulation has been proven to have important practical properties, such as its ability to segment an input image based on its spatial frequencies (change of contrast).

References

[1] P. Rodriguez V., R. Jordan, M. S. Pattichis, M. B. Goens, "Fast AM-FM Demodulation Image and Video Analysis using Single Instruction Multiple Data (SIMD) Architectures" accepted in IASTED International Conference on Signal Processing, Pattern Recognition and Applications (SPPRA 2003).

[2] A. R. Snider, G. A. Serwer, S. B. Ritter "Echocardiography in Pediatric Heart Disease" 2nd ed. 1997, Mosby-Yera Book, Inc..

[3] M. S. Pattichis "AM-FM Transform with Applications" Ph.D. Diss. The University of Texas at Austin 1998.

[4] P. Rodriguez V. "A Radix-2 Multidimensional Transposition-Free FFT Algorithm for Modern Single Instruction Multiple Data (SIMD) Architectures", Proceedings IEEE EUSIPCO 2002

[5] P. Rodríguez V. "A Radix-2 FFT Algorithm for Modern Single Instruction Multiple Data (SIMD) Architectures" Proc. IEEE ICASSP 2002.

[6] J. P. Havlicek, J. W. Havlicek, A. C. Bovik "The Analytical Image" Proceedings IEEE ICIP 1997

[7] P. Rodriguez V., R. Jordan , M. S. Pattichis "Mathematical Morphology operators based on AM-FM Demodulation: Derivation and Applications" to be submitted to IEEE ICASSP 2004

[8] C.I. Christodoulou, E. Kyriacou, M.S. Pattichis, C.S. Pattichis and A. Nicolaides "A Comparative Study of Morphology and Texture Features for the Characterization of Atherosclerotic Carotid Plaques" Proc. IEEE EMBS 2002

[9] J. P. Havlicek, A. C. Bovik Ch. 4.4 "Handbook of Image and Video Processing" Academic Press 2000.